

SUPPLEMENTAL MATERIAL.

Mice and atherosclerosis induction.

To evaluate the influence of immune cell CD69 expression on atherosclerosis development, 5 week old male *Ldlr*^{-/-} CD45.1⁺ mice were irradiated and reconstituted with bone marrow from *cd69*^{-/-} double reporter for Foxp3-mRFP and IL-17A-eGFP²⁴ (*Cd69*^{-/-}*dRep*) mice or WT littermates (*Cd69*^{+/+}*dRep*), both CD45.2⁺. In addition, we generated mixed bone marrow chimeras proficient or deficient for CD69 only in the myeloid or lymphoid compartment; *ldlr*^{-/-} CD45.1⁺ mice were reconstituted with a mix of 75% CD45.2⁺ *Rag2*^{-/-}*γc*^{-/-} BM plus 25% of either *dRep* or *cd69*^{-/-}*dRep* BM (hereafter: LC *Cd69*^{+/+} and LC *Cd69*^{-/-} respectively). After 6 weeks, mice were deemed to be fully reconstituted by phenotyping blood from the tail vein after surface staining with anti-CD45.1 and -CD45.2 antibodies and FACS analysis and were started on a high fat diet (SSNIFF, S9167-E010). Mice were sacrificed at the indicated time points. All animal procedures were approved by the ethics committee of the Comunidad Autónoma de Madrid and conducted in accordance with the institutional guidelines that comply with the European Institutes of Health's; Directive 2010/63/EU of the European Parliament and the Council on the Protection of Animals Used for Scientific Purposes (Official Journal of the European Union. Vol. 53:33-79, 2010).

Monitoring blood Th17, Treg cells and all leukocyte subsets.

To assess the immune response, blood from the tail vein was collected and peripheral blood leukocytes (PBLs) were purified by Ficoll (GE healthcare) gradient. Cells were stimulated in vitro with PMA and ionomycin in the presence

of brefeldin for 4 hours and stained with anti-CD4 APC antibody (BD pharmingen). The percentage of IL-17-eGFP⁺ or Foxp3-RFP⁺ cells in the CD4⁺ population was assessed using a Fortessa (BD Biosciences) flow cytometer, analyses were performed with the FlowJo software. A different group of mice was studied to analyze the kinetics of all leukocyte subsets in blood during high fat diet. PBLs were stimulated overnight with anti-CD3/CD28 for T cell activation or with LPS for the rest. Surface staining with anti-CD44/CD62L was performed to distinguish naïve and memory CD4⁺ T cells and B220 to stain B cells. Myeloid cells were analysed after surface staining with anti-CD11b, -CD11c, -Ly6G/C, -F4/80 and NK cells with anti-Nkp46. The expression of CD69 with anti-CD69 was analysed after stimulation in all the leukocyte subsets by FACS. At the endpoint of the experiment the same process was followed for cells from spleen, non-draining (axillary) lymph nodes and draining (para-aortic) lymph nodes.

LDL isolation, characterization and oxidation. LDL were isolated from pooled plasma of healthy blood volunteers. Plasma was centrifuged to remove chylomicrons, and LDL ($d=1.019-1.063$ g/mL) were isolated by potassium bromide density-gradient ultracentrifugation (36,000 rpm [using a 50.2 Ti rotor, Beckman Coulter] for 18 h at 4 °C). OxLDL were prepared by exposing native LDL (nLDL) to 10 μ M CuSO₄ at 37 °C. The degree of oxidation was monitored by fluorescent emission at 234 nm. Thiobarbituric acid-reactive substances (TBARS) content was used as an indirect evaluation of lipid peroxidation (nLDL<1.0 nmol malondialdehyde (MDA)/mg of LDL protein; oxLDL>20 nmol MDA/mg LDL protein). The absence of contamination by other lipoproteins was determined by electrophoresis on agarose gels (Paragon Electrophoresis system, Beckman). The content of protein (BCA protein assay) and cholesterol

(Cholesterol assay kit, RefLab) was determined by colorimetric assays. LDL were sterilized by filtration through a low protein-binding non-pyrogenic filter. Endotoxin contamination was discarded by the chromogenic Limulus amoebocyte assay. Lipoproteins were stored under N₂ at 4 °C in the dark. Fluorescent labelling of the lipid moiety of lipoproteins was performed by incubating lipoproteins with Dil (1,1'-dioctadecyl-3,3,3',3'-tetramethylindo-carbocyanine perchlorate) at 37 °C for 8 h. Labelled lipoproteins were re-floated by ultracentrifugation, dialyzed and sterilized.

Lipoprotein Binding and Internalization Assays. Binding and cell association of Dil-labeled lipoproteins to Jurkat (JKwt Vs JKCD69) and RBL-2H3 (RBLwt Vs RBLCD69) cells were performed by incubating 5x10⁵ cells with 10 µg/ml of Dil-labeled lipoprotein in culture medium supplemented with 10% (v/v) fetal bovine serum deprived of lipoproteins (LPDS) for 2h at 4°C (binding) or 37°C (cell association). After incubation, cells were washed in cold PBS and analyzed by fluorescence flow cytometry using a FACScalibur® cytofluorometer (Becton Dickinson, Mountain View, CA). For blocking assays, unlabeled-lipoprotein or purified antibodies (50 µg/ml) were pre-incubated for 30 min in incomplete medium supplemented with 10 % (v/v) LPDS. For internalization assays, Jurkat cells (JKwt and JKCD69) were incubated with unlabelled oxLDL (50 µg/ml) at different time points (10, 30, 60, 90, 120 and 240 minutes) in culture medium supplemented with 10% (v/v) LPDS and CD69 expression on membrane surface was analyzed by flow cytometry.

RT-PCR. Jurkat cells (JKwt and JKCD69) 1x10⁶/ml were incubated in the presence of PMA (50 µg/ml) and ionomycin (0.5 µg/ml) for 4 h, then cells were washed twice and incubated in the presence or absence of oxLDL (50 µg/ml)

during 2 h. Cells were then harvested and processed for RNA isolation. Total RNA was isolated with a QIAGEN RNeasy Kit (QIAGEN). Then 1 µg/ml of total RNA was reverse transcribed into cDNA, PCR were performed using SYBR Green. Data were normalized using GAPDH expression. Data were analyzed using 2-ΔΔCt method. GAPDH forward: 5'-GCC CAA TAC GAC CAA ATC C-3'; GAPDH reverse: 5' AGC CAC ATC GCT CAG ACA C3'. IL-8 forward: 5'-TCT GTG TGA AGG TGC AGT TTT G-3'; IL8 reverse: 5'-GGG GTG GAA AGG TTT GGA GT-3'. For the expression of NR4A nuclear receptors, Jurkat cells (JKwt and JKCD69) 1x10⁶ cell/ml were incubated with oxLDL (50 µg/ml) at different time points. For blocking assays, cells were pre-incubated with anti-CD69 (20 µg/ml) during 45 min. RT-PCR for human and mouse NR4A receptors was performed using Taqman assays (Applied Biosystems).

Human CD4⁺ T cell polarization. For human Th1, Th17 and Treg polarization, CD4⁺ T cells were purified by immunomagnetic depletion with the human CD4⁺ T Cell Isolation Kit II (Miltenyi Biotec, CA, USA) with a purity >96%. Th17 cells were polarized as described. For Th1 polarization CD4⁺ T cells (1 x 10⁶), were incubated with IL-2 (20 U/ml) and IL-12 (20 ng/ml), while for Treg polarization cells were cultured with TGF-β (5 ng/ml) and IL-2 (20 U/ml) (all cytokines from R&D systems). After 5 days of culture, percentage of IFN-γ and IL-2 producing cells (Th1) and Foxp3⁺ CD25⁺ cell (Treg) was analyzed in a FACS Canto Cytometer and analyzed with FlowJo software. Where indicated, oxLDL (50 µg/ml) and anti-CD69 (20 µg/ml) were added to the cultures.

Tissue processing and immunohistochemistry

For plaque area assessment, 5 µm thick sections at 100 µm intervals were collected starting at the origin of the aortic valve cusps. Sections were stained

with Oil Red O (ORO) staining, (Sigma-Aldrich) and hematoxylin, and lesion size was analyzed with ImageJ software. For Masson trichrome staining 7 μm thick sections at 100 μm intervals were collected. Sections were stained with the Masson-Goldner staining kit (Merck). For specific staining, anti-F480 antibody was purchased from Abcam (ab6640) and anti-CD3 from Santa Cruz Biotechnology (sc-1127).

Supplementary Table 1: Demographic characteristics and cardiovascular risk factors.

	Total	No Atherosclerosis	Focal Disease	Generalized Disease	P-value
	(n=305)	(n=122)	(n=55)	(n=128)	
Age (years)	48,58 ± 3,9	46,66 ± 3,5	50,84 ± 2,2	49,46 ± 4	<0,001
Sex (men)	308 (100)	122 (100)	55 (100)	128 (100)	-
Family history of CVD	54 (17,5)	17 (13,9)	6 (10,9)	31 (24,2)	0,02
Smoking	84 (27,3)	24 (19,7)	10 (18,2)	49 (38,3)	<0,001
BMI (Kg/m²)	27,46 ± 3,3	27,46 ± 3,4	27,21 ± 3,4	27,52 ± 3,3	0,485
Weight (kg)	83,5 ± 12,1	84,19 ± 12,6	82,28 ± 11,2	83,02 ± 12,1	0,749
Height (cm)	174,2 ± 6,6	174,9 ± 7	173,9 ± 6,7	173,5 ± 5,9	0,095
Obesity	60 (19,5)	24 (19,7)	10 (18,2)	25 (19,5)	0,993
Hypertension	78 (25,3)	27 (22,1)	12 (21,8)	37 (28,9)	0,19
SBP (mmHg)	121,8 ± 12,5	121,1 ± 13,7	119,1 ± 10,9	123,7 ± 11,4	0,005
DBP (mmHg)	76,13 ± 9,1	75,3 ± 10,6	75,47 ± 8,6	77,18 ± 7,5	0,033
Diabetes	13 (4,2)	0 (0)	1 (1,8)	11 (8,6)	<0,001
Fasting glucose (mg/dL)	93 [87 - 100]	93 [87 - 97]	93 [88 - 99]	94 [87 - 103]	0,068
HbA1c (%)	5,5 [5,3 - 5,8]	5,5 [5,2 - 5,7]	5,4 [5,3 - 5,8]	5,5 [5,3 - 5,9]	0,004
Insulin (uU/mL)	6,2 [4,2 - 9,2]	5,9 [4,1 - 9,1]	6,4 [4,6 - 9,3]	6,35 [4,2 - 9,5]	0,887
Dyslipidemia	196 (63,6)	71 (58,2)	34 (61,8)	89 (69,5)	0,059
Total cholesterol (mg/dL)	202,1 ± 32,7	199,8 ± 28,9	200,5 ± 38,5	205,8 ± 33	0,151
LDL-C (mg/dL)	136,2 ± 27,8	135,1 ± 24,6	135,7 ± 32,8	138,2 ± 28,3	0,411
HDL-C (mg/dL)	42,79 ± 9,6	42,63 ± 9,3	44,11 ± 9,1	42,51 ± 9,9	0,71
Triglycerides (mg/dL)	97 [73 - 139]	91 [69 - 139]	89 [71 - 122]	106 [75 - 144]	0,017
Oxidized LDL-C(mg/dL)	54,13 ± 16,1	52,11 ± 13,9	52,35 ± 18,4	56,86 ± 16,8	0,027
Lipoprotein a (mg/dL)	16,6 [6,64 - 38,6]	12,4 [4,76 - 27,4]	15,4 [8,13 - 40]	20,6 [7,92 - 45,5]	0,016
Creatinine (mg/dL)	0,89 ± 0,1	0,91 ± 0,1	0,91 ± 0,1	0,86 ± 0,1	0,005
Cystatin C (mg/L)	0,78 ± 0,1	0,78 ± 0,1	0,79 ± 0,1	0,77 ± 0,1	0,226
Fibrinogen (mg/dL)	265,6 ± 45,2	256 ± 36,7	263,4 ± 45,2	274,5 ± 50,2	0,248
P-Selectin (ng/mL)	140,3 ± 43,3	136,8 ± 40,8	142,4 ± 39,2	142,3 ± 47	0,001
hs-CRP (mg/mL)	0,13 [0,07 - 0,22]	0,13 [0,06 - 0,20]	0,13 [0,08 - 0,21]	0,135 [0,07 - 0,124]	0,364
VCAM-1 (ng/mL)	620 [494,8 - 760,6]	620 [505 - 763]	672 [520,5 - 841,5]	612,8 [483,1 - 725,4]	0,277
PREDIMED	4,92 ± 1,42	4,83 ± 1,48	5,15 ± 1,33	4,90 ± 1,40	0,711
MVPA	51,48 ± 21,41	49,50 ± 18,83	57,25 ± 24,89	50,94 ± 21,90	0,632

Data are expressed as mean±SD, median and IQR or n (%). P-values are derived from Anova for log-transformed continuous variables and chi-square for categorical variables, except for those variables with n<6 for which Fisher Test was used. BMI: Body mass index. CVD: Cardiovascular Disease; SBP: Systolic blood pressure; DBP: Diastolic blood pressure; LDL-C: Low-density lipoprotein cholesterol; HDL-C: High-density lipoprotein cholesterol. MVPA: Moderate to Vigorous Physical Activity. In bold, variables included in the multivariable model.

Supplementary Table 2: Univariable logistic regression to compare individuals with “Generalized subclinical atherosclerosis” to individuals with “no disease”.

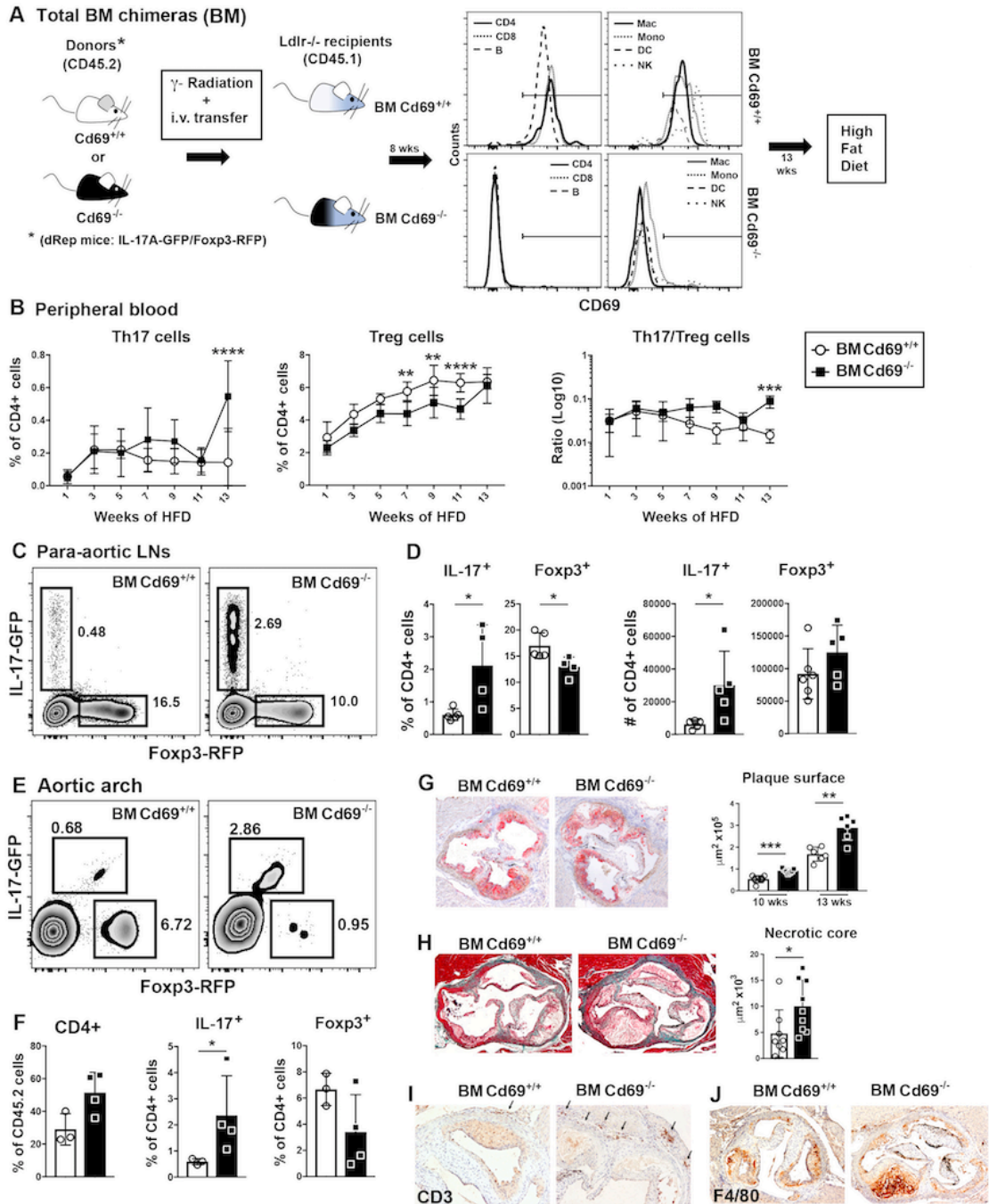
	OR (95% CI)	P Value
log2(CD69)	0.63(0.46-0.85)	0.0035
log2(NR4A1)	0.69(0.53-0.88)	0.0031
Age	1.21(1.13-1.31)	0.0000
FH	1.97(1.04-3.86)	0.0412
Smoking	2.53(1.44-4.54)	0.0014
Hypercholesterolemia	1.64(0.98-2.77)	0.0628
Hypertension	1.43(0.81-2.56)	0.2209
Diabetes*	NA	0.0001
BMI	1.01(0.93-1.08)	0.8928
Monocytes	11.57(1.61-89.99)	0.0168
Lymphocytes	3.08(1.8-5.5)	0.0001
Leukocytes	1.66(1.37-2.04)	0.0000
Neutrophils	1.91(1.47-2.55)	0.0000
oxLDL	1.02(1-1.04)	0.0170

*For diabetes, no OR could be estimated due to the lack of individuals with diabetes in the “No disease” group (see Supplementary Table 1). P-value for diabetes was estimated using the likelihood ratio test.

Supplementary Table 3. Correlation between the expression level of CD69 (log2 scaled) and a set of relevant molecular and clinical variables.

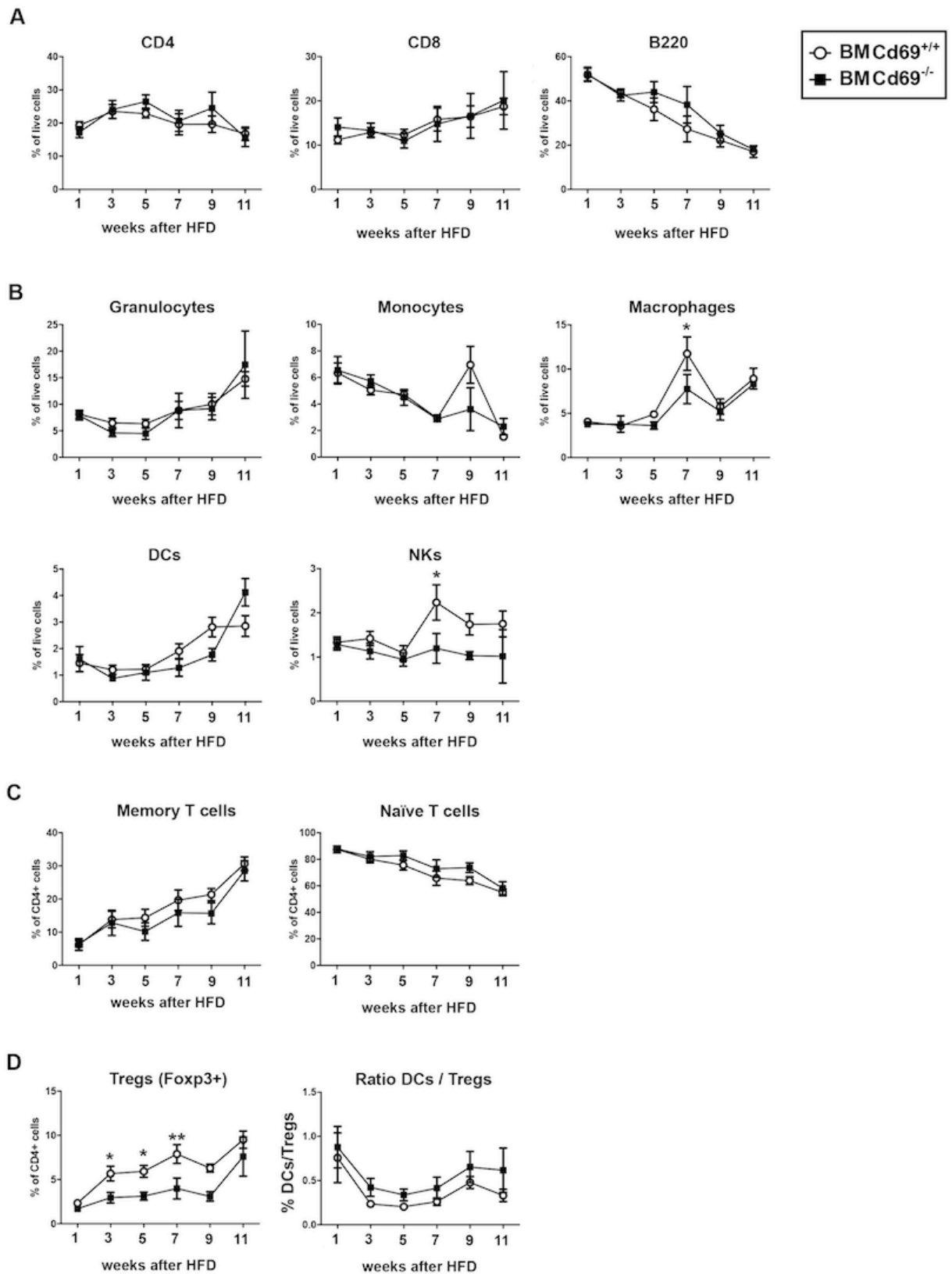
	Estimate*	P Value
log2(NR4A1)	0.36	0.0000
Age	0.00	0.9170
FH	-0.09	0.5190
Smoking	-0.28	0.0266
Hypercholesterolemia	-0.08	0.4930
Hypertension	0.00	0.9950
Diabetes	-0.35	0.1970
BMI	-0.02	0.3660
Monocytes	0.13	0.7720
Lymphocytes	0.16	0.1390
Leukocytes	-0.03	0.3950
Neutrophils	-0.09	0.0564
oxLDL	-0.01	0.0520
CRP	0.03	0.9190
FH10Y	-1.32	0.2650

* For continuous independent variables the *Estimate* represents the slope of the linear regression fit. For discrete independent variables the *Estimate* represents the difference in expression between the groups.



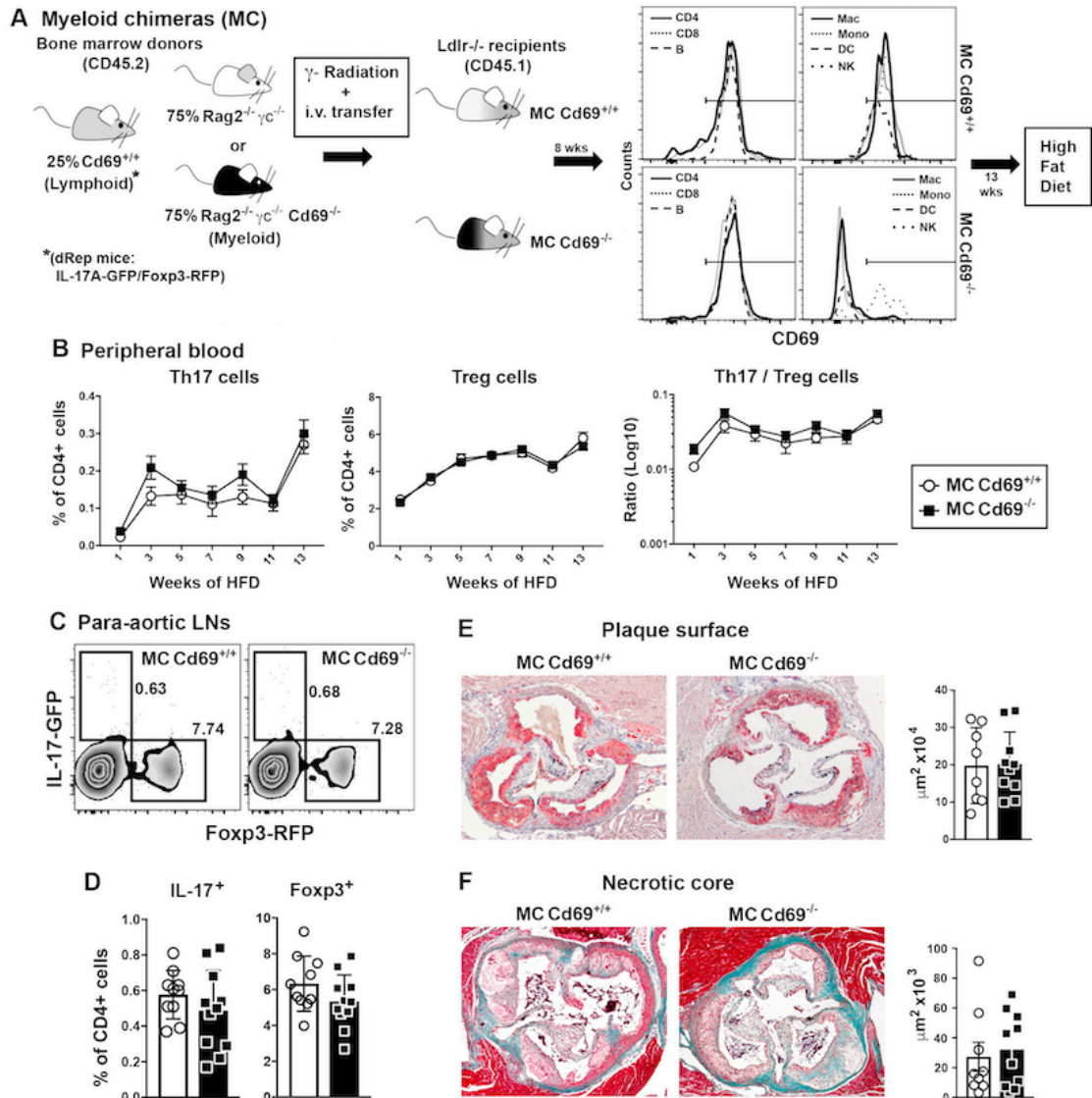
Supplementary Figure 1. CD69 regulates adaptive immune responses in HFD conditions. **A.** Ldlr^{-/-} mice were lethally irradiated and reconstituted with bone marrow from C57BL/6 Cd69^{+/+} or Cd69^{-/-} dRep mice. Eight weeks after reconstitution PBMCs were > 90% CD45.2⁺. Reconstitution of lymphoid and myeloid compartments of CD45.2⁺ cells was assessed by FACS. Histograms show CD69 expression on CD4 and CD8 T cells, B cells (B), macrophages (Mac),

monocytes (Mono), dendritic cells (DC) and natural killer cells (NK). PBMCs were stimulated with anti-CD3/CD28 for lymphoid cells and LPS for myeloid cells, of the indicated groups. **B.** Percentage of Th17 (IL-17-GFP⁺), Treg (Foxp3-RFP⁺) CD4⁺ T cells and Th17/Treg ratio in peripheral blood leukocytes of BM Cd69^{+/+} and BM Cd69^{-/-} mice at the indicated time points after HFD initiation. Error bars show SEM, ** $P < 0.01$, *** $P < 0.001$, **** $P < 0.0001$. P values were calculated by 2-way repeated-measures ANOVA (Sidak's *post hoc* test). **C.** Flow cytometry analysis of Th17 and Treg cells in para-aortic lymph nodes of BM Cd69^{+/+} and BM Cd69^{-/-} mice at 10 weeks after HFD administration, n=12 mice per group. **D.** Percentages and absolute numbers of Th17 and Treg cells from para-aortic lymph nodes of BM Cd69^{+/+} and BM Cd69^{-/-} mice 10 weeks after HFD administration, n=12 mice per group. Error bars show SEM, * $p < 0.05$, as determined by unpaired *t*-test or Mann-Whitney U test. **E.** Flow cytometry analysis of aortic arch 13 weeks after HFD initiation. **F.** Quantification and statistical analysis of data shown in E, n=7 mice per group, * $P < 0.05$, as determined by Mann-Whitney U test. **G.** Lack of CD69 on immune cells accelerates atheroma plaque formation. Oil Red O staining in aortic valves from BM Cd69^{+/+} and BM Cd69^{-/-} mice after 13 weeks of HFD (left) and quantification of plaque surface at the indicated time points (right), n=16 mice per group pooled from 3 different experiments. **H.** As before, Masson trichrome staining and quantification of fibrosis and necrotic core after 13 weeks of HFD, n=6 mice/group Error bars show SEM, * $P < 0.05$, ** $P < 0.01$, *** $P < 0.001$, as determined by unpaired *t*-test. **I.** As before, F4/80 staining. **J.** As before, CD3 staining, C and D. representative images of 6 mice/group. Original magnifications: A-C: 4x, D: 10x.



Supplementary figure 2. Analysis of blood leukocyte subsets during high fat diet. The percentages of peripheral blood leukocyte subsets were analyzed during HFD administration. **A.** Analysis of lymphoid CD4⁺, CD8⁺ T cells and B

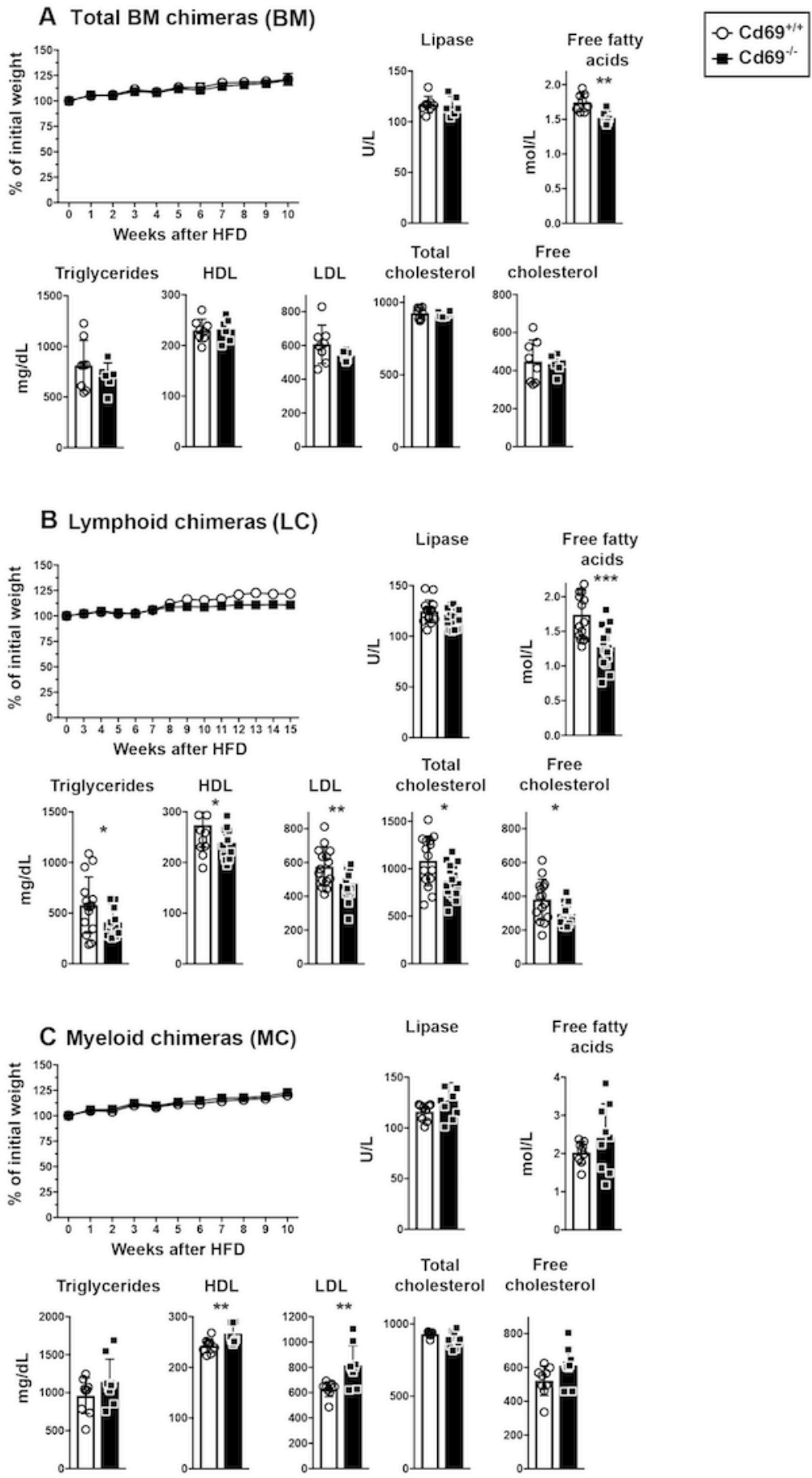
cells (B220) was performed by FACS. **B.** Myeloid cells were analysed after surface staining with anti-CD11b, -CD11c, -Ly6G/C, -F4/80 and NK cells with anti-Nkp46. The percentages of granulocytes, monocytes, macrophages, natural killer cells (NKs) and dendritic cells (DCs) are shown. **C.** Surface staining with anti-CD44/CD62L was performed to distinguish naïve ($CD62L^{hi} CD44^{lo}$) and memory ($CD62L^{lo} CD44^{hi}$) $CD4^{+}$ T cells. **D.** Percentages of Tregs (Foxp3+) and the ratio between DCs and Tregs is shown. $n = 15$ BM $Cd69^{+/+}$ and $n = 13$ BM $Cd69^{-/}$ -chimeric mice. Error bars show SEM, $*P < 0.05$, $**P < 0.01$. P values were calculated by 2-way ANOVA (Sidak's *post hoc* test).



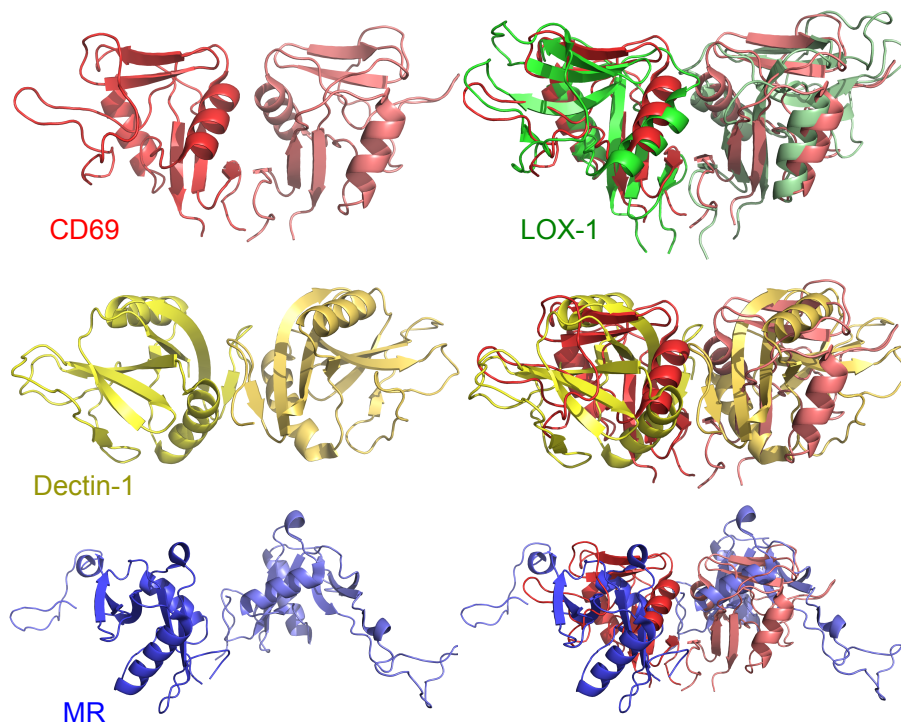
Supplementary figure 3. CD69 deficiency in myeloid cells does not influence atherosclerosis development. **A.** Scheme illustrating the generation of myeloid chimeras (MC). Ldlr^{-/-} mice were lethally irradiated and reconstituted with mixed bone marrow, from Rag2^{-/-}γc^{-/-} or Rag2^{-/-}γc^{-/-}Cd69^{-/-} plus bone marrow from C57BL/6-CD69^{+/+} (double-reporter dRep: IL-17-GFP⁺ / Foxp3-RFP⁺) at a 3:1 ratio, respectively. Eight weeks after reconstitution PBMCs were > 90% CD45.2⁺. Reconstitution of lymphoid and myeloid compartments of CD45.2⁺ cells was assessed by FACS. Histograms show CD69 expression on CD4 and CD8 T cells, B cells (B), macrophages (Mac), monocytes (Mono),

dendritic cells (DC) and natural killer cells (NK). PBMCs were stimulated with anti-CD3/CD28 for lymphoid cells and LPS for myeloid cells, of the indicated groups.

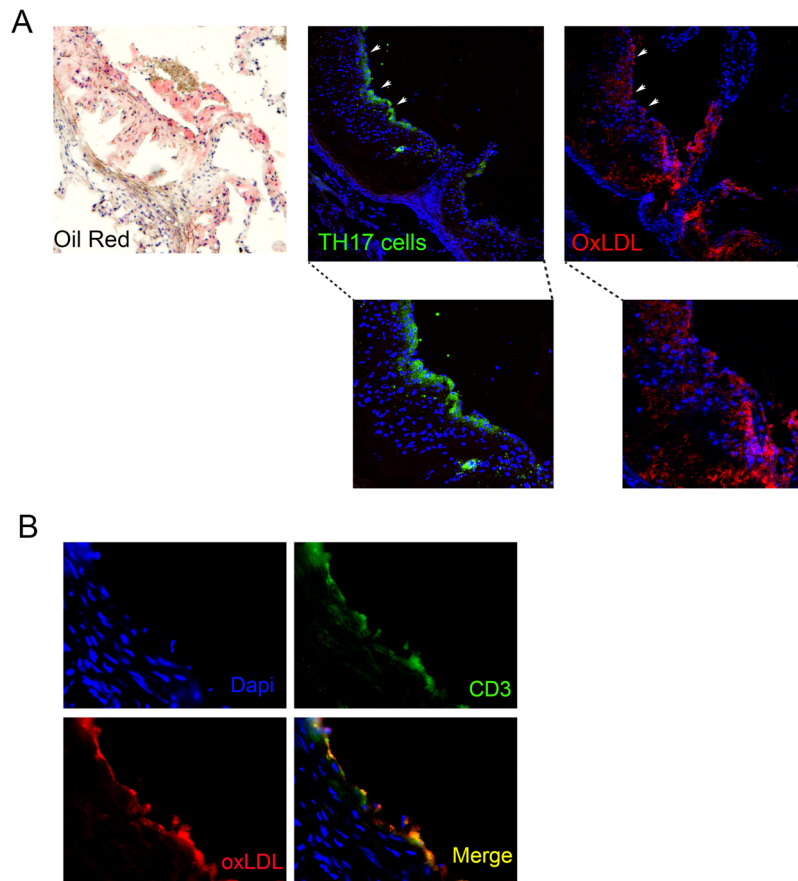
B. Kinetics of the adaptive immune response in peripheral blood for Th17 (IL-17-GFP⁺), Treg (Foxp3-RFP⁺) CD4⁺ T cells and Th17/Treg ratio in peripheral blood leukocytes after HFD, n=11 mice/group, **C.** Flow cytometry analysis of Foxp3-mRFP⁺ and IL-17-eGFP⁺ CD4 T cells in para-aortic LNs of MC *Cd69*^{+/+} and MC *Cd69*^{-/-} mice after 13 weeks of HFD, **D.** Quantification and statistical analysis of data shown in C, n=12 mice per group, **E.** Oil Red O staining and quantification of plaque in aortic valves from MC *Cd69*^{+/+} and MC *Cd69*^{-/-} mice after 13 weeks of HFD, n= 8-10 mice/group, **F.** As in E., Masson trichrome staining and necrotic core quantification, n=8-10 mice/group Original magnifications: 4x. Error bars show SEM. No significant differences were observed between groups as determined by two-way repeated-measures ANOVA (Sidak's multiple comparisons *post hoc* tests) (B), unpaired *t*-test and Mann-Whitney U test (D-F) as appropriate.



Supplementary Figure 4. Analysis of circulating lipids in mice lacking CD69 in total immune, lymphoid or myeloid compartments. Weight gain, lipase activity, free fatty acids, triglyceride and cholesterol levels of the indicated experimental groups were measured. **A.** Weight curve and biochemical profile of chimeric BM *Cd69^{+/+}* and BM *Cd69^{-/-}* mice, n=6-8 mice/group. **B.** as in a, for LC *Cd69^{+/+}* and LC *Cd69^{-/-}* mice, n=15-16 mice/group. **C.** as in A for MC *Cd69^{+/+}* and MC *Cd69^{-/-}* mice, n=9 mice/group. No significant differences were observed in weight gain between groups as determined by two-way repeated-measures ANOVA (Sidak's multiple comparisons *post hoc* tests). Error bars show SEM. **P* < 0.05, ***P* < 0.01, ****P* < 0.001, as determined by unpaired *t*-test and Mann-Whitney U test as appropriate.



Supplementary Figure 5: The dimeric structures of C-type lectin structures. Ribbon representations of the CD69 (PDB code 1E8I), Dectin-1 (PDB code 2BPD) and the macrophage mannose receptor (MR, PDB code 1EGG) CTLD structures (left panels). Superimposed LOX-1 (PDB code 1YXK), Dectin-1 and MR structures on the CD69 dimer are shown on the right. Prepared with PyMOL.



Supplementary Figure 6: Localization of oxLDL and T cells in atheroma plaque.

A. Lipids, Th17+ T cells and oxLDL in atheroma plaque in aortic valves. Oil Red O staining was used to identify lipids. Endogenous GFP-Th17+ T cells and oxLDL were detected in serial tissue sections of aortic valves from WT *Cd69^{+/+}* mice after 16 weeks of HFD. **B.** Co-localization of CD3+ T cells and oxLDL in atheroma plaque